Biallelic mutations in KDSR disrupt ceramide synthesis and result in a spectrum of keratinization disorders associated with thrombocytopenia

Journal:	*Journal of Investigative Dermatology*
Manuscript ID	Draft
Article Type:	Original Article
Date Submitted by the Author:	n/a
Complete List of Authors:	Takeichi, Takuya; Nagoya University Graduate School of Medicine, Dermatology Lee, John; King's College London, Dermatology Ohno, Yusuke; Hokkaido University, Faculty of Pharmaceutical Sciences Torrelo, Antonio ; Hospital del Niño Jesús, Department of Dermatology Lozano, Maria; Universidad de Murcia, Servivio de Hematologia y Oncologia Medica Kihara, Akio; Hokkaido University, Pharmaceutical Sciences Liu, Lu; The Robin Eady National Diagnostic Epidermolysis Bullosa Laboratory, Guys & St Thomas' Hospital NHS FT, Molecular laboratory Yasuda, Yuka; Kao Corporation, Analytical Science Research Laboratories Ishikawa, Junko; Kao corporation, Biological Science Lab. Murase, Takatoshi; Kao corporation, Biological Science Lab. Rodrigo, Ana; Hospital de Alta Resolucion Sierra de Segura, Dermatology Fernandez-Crehuet, Pablo; Hospital Universitario Reina Sofia, Dermatology Toi, Yoichiro; Hiroshima Shiritsu Hiroshima Shimin Byoin, Dermatology Mellerio, Jemma; St John's Institute of Dermatology, Genetic Skin Disease Group Rivero, Jose; Universidad de Murcia, Servivio de Hematologia y Oncologia Medica Vicente, Vicente; Universidad de Murcia, Servivio de Hematologia y Oncologia Medica Kelsell, David; Queen Mary University of London, Blizard Institute; Nishimura, Yutaka; Hiroshima Shiritsu Hiroshima Shimin Byoin, General Perinatology Okuno, Yusuke; Nagoya Daigaku Igakubu Fuzoku Byoin, Advanced medicine and Clinical Research Kojima, Daiei; Nagoya Daigaku Daigakuin Igakukei Kenkyuka Igakubu, Pediatrics Ogawa, Yasushi; Nagoya University Graduate School of Medicine, Dermatology Sugiura, Kazumitsu; Fujita Health University School of Medicine, Department of Dermatology Simpson, Michael; King's College London, Medical and Molecular Genetics McLean, Irwin; University of Dundee, Dermatology and Genetic Medicine Akiyama, Masashi; Nagoya University Graduate School of Medicine,

	Department of Dermatology McGrath, John; St. John's Institute of Dermatology, Genetic Skin Disease Group;
Key Words:	keratoderma, ichthyosis, ceramide, thrombocytopenia, KDSR

SCHOLARONE™
Manuscripts

For Review Only

Biallelic mutations in *KDSR* disrupt ceramide synthesis and result in a spectrum of keratinization disorders associated with thrombocytopenia

Takuya Takeichi[1,2], Antonio Torrelo[3], John Y. W. Lee[1], Yusuke Ohno[4], María Luisa Lozano[5,6], Akio Kihara[4], Lu Liu[7], Yuka Yasuda[8], Junko Ishikawa[9], Takatoshi Murase[9], Ana Belén Rodrigo[10], Pablo Fernández-Crehuet[11], Yoichiro Toi[12], Jemima Mellerio[1,13], José Rivera[5], Vicente Vicente[5], David P. Kelsell[14], Yutaka Nishimura[15], Yusuke Okuno[16,17], Daiei Kojima[17], Yasushi Ogawa[2], Kazumitsu Sugiura[18], Michael A. Simpson[19], W. H. Irwin McLean[20], Masashi Akiyama[2], John A. McGrath[1,20]

1. St John's Institute of Dermatology, King's College London (Guy's Campus), London, UK
2. Department of Dermatology, Nagoya University Graduate School of Medicine, Nagoya, Japan
3. Department of Dermatology, Hospital Infantil del Niño Jesús, Madrid, Spain
4. Faculty of Pharmaceutical Sciences, Hokkaido University, Sapporo, Japan
5. Centro Regional de Hemodonación, Servicio de Hematología y Oncología Médica, Hospital Universitario Morales Meseguer, IMIB-Arrixaca, Universidad de Murcia, Spain
6. Centro de Investigación Biomédica en Red de Enfermedades Raras (CIBERER), Instituto de Salud Carlos III (ISCIII) Madrid, Spain
7. Viapath, St Thomas' Hospital, London, UK
8. Analytical Science Research Laboratories, Kao Corporation, Haga, Tochigi, Japan
9. Biological Science Research Laboratories, Kao Corporation, Haga, Tochigi, Japan

For Review Only

10. Department of Dermatology, Hospital Sierra de Segura, Puente de Génave, Jaén, Spain
11. Department of Dermatology, Hospital Universitario Reina Sofía, Córdoba, Spain
12. Department of Dermatology, Hiroshima City Hiroshima Citizens Hospital, Hiroshima, Japan
13. Department of Dermatology, Great Ormond Street Hospital for Children NHS Foundation Trust, London, United Kingdom
14. Centre for Cell Biology and Cutaneous Research, Blizard Institute, Barts and the London School of Medicine and Dentistry, Queen Mary University of London, Whitechapel, London, UK
15. Department of General Perinatology, Hiroshima City Hiroshima Citizens Hospital, Hiroshima, Japan
16. Center for Advanced Medicine and Clinical Research, Nagoya University Hospital, Nagoya, Japan
17. Department of Pediatrics, Nagoya University Graduate School of Medicine, Nagoya, Japan
18. Department of Dermatology, Fujita Health University School of Medicine, Toyoake, Japan
19. Department of Medical and Molecular Genetics, King's College London, School of Medicine, Guy's Hospital, London, UK
20. Centre for Dermatology and Genetic Medicine, Division of Molecular Medicine, University of Dundee, Dundee, UK

For Review Only

Corresponding author: John A. McGrath, Dermatology Research Labs, Floor 9 Tower Wing, Guy's Hospital, Great Maze Pond, London SE1 9RT, United Kingdom. Tel: 44-2071886409; Fax: 44-2071888050; E-mail: john.mcgrath@kcl.ac.uk

Short title: *KDSR* mutations in a disorder of keratinization and thrombocytopenia

Keywords: Keratoderma, ichthyosis, thrombocytopenia, KDSR, ceramide.

Abbreviations: KDSR, 3-ketodihydrosphingosine reductase; WES, whole-exome sequencing.

For Review Only

ABSTRACT

Mutations in ceramide biosynthesis pathways have been implicated in a few Mendelian disorders of keratinization although ceramides are known to have key roles in several biological processes in skin and other tissues. Using whole-exome sequencing in four unrelated probands with undiagnosed skin hyperkeratosis/ichthyosis, we identified compound heterozygosity for mutations in *KDSR*, encoding an enzyme in the *de novo* synthesis pathway of ceramides. Two individuals had hyperkeratosis confined to palms and soles as well as anogenital skin, whereas the other two had more severe, generalized Harlequin ichthyosis-like skin. Of note, thrombocytopenia was present in all cases. The mutations in *KDSR* were associated with reduced ceramide levels in skin and impaired platelet function. KDSR enzymatic activity was variably reduced in all cases resulting in defective acylceramide synthesis, more so for the Harlequin ichthyosis cases, thus providing a basis for genotype-phenotype correlation. This study demonstrates that biallelic mutations in *KDSR* are implicated in an extended spectrum of disorders of keratinization in which thrombocytopenia is also part of the phenotype. Mutations in *KDSR* cause defective ceramide biosynthesis, underscoring the importance of ceramide and sphingosine synthesis pathways in skin and platelet biology.

For Review Only

INTRODUCTION

The hereditary palmoplantar keratodermas and ichthyoses comprise a heterogeneous collection of genodermatoses caused by mutations in >100 genes involved in a multitude of biologic pathways and processes (Oji et al., 2010; Sakiyama and Kubo, 2016). Despite major advances in discovering the underlying molecular genetic basis of many of these disorders, several cases remain unresolved, indicating the likely contribution of further gene pathology (Fischer, 2009).

In this study, we investigated four unrelated individuals from Spain, Japan and the United Kingdom who presented with inherited disorders of keratinization. The two patients from Spain displayed a milder phenotype of palmoplantar and anogenital hyperkeratosis, whereas the other two cases had a more severe phenotype resembling Harlequin ichthyosis. An additional feature, present in all subjects, was a reduction in the number of blood platelets (thrombocytopenia). Using whole-exome sequencing, functional studies on skin and platelets, as well as *in vitro* analyses, we identify autosomal recessive mutations in *KDSR*, encoding 3-ketodihydrosphingosine reductase, which catalyzes the reduction of 3-ketodihydrosphingosine (KDS) to dihydrosphingosine (DHS), as being responsible for the skin and platelet abnormalities, thus expanding the clinical pathology associated with ceramide biosynthesis pathways.

RESULTS

Clinical features of individuals with *KDSR* mutations

Patient 1 is a 15-year-old male and the only child of unrelated healthy parents (Family 1; see **Figure 1a**). His parents are originally from the same geographic area in mid-

For Review Only

southeast Spain. Since the age of 12 months, he developed palmoplantar hyperkeratosis with extension to the dorsae of the hands and feet, wrists and ankles (**Figure 2**), as well as anogenital hyperkeratosis and erythema. Aged 2 years, a blood count was performed because of mucocutaneous bleeding, which revealed a severe, isolated thrombocytopenia (platelets < $30x10^9$/L; bone marrow biopsy showed a normal to increased number of megakaryocytes only). A diagnosis of primary immune thrombocytopenia was made but treatment with oral corticosteroids was suboptimal. Splenectomy aged 11 years led to a slight increase in platelets (~$40x10^9$/L) although clinically he continues to suffer recurrent nose bleeds. Light microscopy of lesional skin revealed non-specific findings of psoriasiform acanthosis and focal hypergranulosis but no epidermolytic changes.

Patient 2 is a 21-year-old male and the older of two brothers born to healthy unrelated parents (Family 2; **Figure 1b**). He is the only affected individual among his relatives. This family originates from the same geographic region in Spain as Family 1, but the pedigrees are not known to be related. Aged 15 months, he developed diffuse hyperkeratosis on the palms and soles, without progression to the dorsae of hands or feet (i.e. less severe than Patient 1). He also developed perianal erythema and hyperkeratosis. In addition, he suffered episodes of bruising with evidence of isolated thrombocytopenia. Bone marrow studies showed normal hematologic morphology. At present, he has not manifested clinically relevant signs of bleeding despite persistently low platelets (~$20x10^9$/L).

Patient 3 was the second child born to unrelated white Caucasian parents from the United Kingdom (Family 3; **Figure 1c**). His parents, older brother, and all other relatives were healthy. His mother's pregnancy was uneventful until the last trimester when oligohydramnios was noted. She had spontaneous rupture of membranes at 33+5 weeks and underwent elective cesarean section at 35+2 weeks with an infant birth weight of 2.74

For Review Only

kg. At birth, the patient was covered in thick adherent plate-like scales with prominent ectropion and eclabium, and pinching of all digits, collectively consistent with Harlequin ichthyosis. He was treated in a humidified incubator with hourly greasy emollients and lubricating eye drops. Acitretin was started which led to some reduction in adherent scaling, although he developed pseudomonas septicemia aged 15 days and further sepsis thereafter. At birth, platelet count was $120x10^9$/L but within 2 weeks this dropped to $50x10^9$/L, and by the 3rd week to ~$20\text{-}30x10^9$/L and remained at this level. At day 36, he deteriorated clinically with tachypnea and hypotension associated with a profound metabolic acidosis. Despite efforts to resuscitate him, he died aged 37 days.

Patient 4 is a 6-year-old Japanese male and is the younger of two brothers born to unrelated parents (Family 4; **Figure 1d**). His mother and brother have atopic dermatitis, but there is no other noteworthy family history. He was delivered at 35+3 weeks by normal spontaneous vaginal delivery with a birth weight of 1.9 kg. At birth, he had thick plate-like scales with deep fissuring overlying erythrodermic skin. Severe eclabium and ectropion were also observed. Skin biopsy revealed severe hyperkeratosis with parakeratosis. These features were consistent with Harlequin ichthyosis. He was treated in the neonatal intensive care unit but did not receive systemic retinoids. Over the first 2 months of life, the thick scales desquamated gradually, resulting in generalized erythroderma and fine scaling. Platelet count was normal at birth ($140\text{-}150x10^9$/L) but since the age of 2 months this progressively decreased, and at 3 years of age he had severe thrombocytopenia ($4\text{-}11x10^9$/L).

Identification of compound heterozygous mutations in *KDSR* in all affected individuals

For Review Only

After ethics' committee approval and written informed consent, whole-exome sequencing (WES) was performed using DNA from all affected probands. Candidate gene mutations were prioritized by filtering for variants with a frequency of less than 0.1% in public databases such as the Exome Aggregation Consortium (ExAC), Exome Variant Server (EVS), 1000 Genomes Project and an in-house repository. Of note, WES failed to reveal any pathogenic mutations in genes already implicated in ichthyosis or palmoplantar keratoderma. Strikingly, all four affected individuals harbored rare compound heterozygous mutations in *KDSR,* encoding 3-ketodihydrosphingosine reductase (**Figure 1e** and **Table 1**). The mutations were verified by Sanger sequencing and segregated with disease status in family members whose DNA was available (**Figures 1a-d**). Our study revealed three missense mutations (p.Phe138Cys; p.Gly182Ser; p.Gly271Glu), one synonymous variant (c.879G>A, p.Gln293Gln, but affecting the last base of an exon and therefore potentially a donor splice site mutation), one other splice site mutation (c.417+3G>A), and one out-of-frame deletion (c.223_224delGA, p.Glu75Asnfs*2) (**Figure 1e**). Although the two Spanish cases (Patients 1 and 2) were not thought to be related, they were both compound heterozygotes for the same mutations in *KDSR*, and we demonstrated that the incidence of both pathogenic changes (p.Phe138Cys and c.417+3G>A) is likely to represent shared ancestral alleles within these families and potentially other individuals within this part of Spain (**Supplementary Table S1** online). The splicing mutation (c.417+3A>C) was predicted to cause a reduction of 41.8% of transcripts expressing exon 5 of *KDSR*, based on the SPANR tool (Xiong et al., 2015), which was confirmed by RT-PCR using RNA extracted from skin (Patients 1 and 2). Sequencing of cDNA from exon 2 to exon 7 of *KDSR* demonstrated skipping of exon 5 (96-bp, Δ5) and skipping exons 5 and 6 (288-bp, Δ5Δ6) (data not shown). Both of these truncated transcripts restore the reading frames. The synonymous c.879G>A

For Review Only

mutation (p.Gln293Gln) was predicted to lead to loss of exon 10 with retention of 15 base pairs from intron 9 (Δ10+VSSA), although cDNA was not available for verification.

***KDSR* mutations impair enzymatic activity and lead to defective acylceramide synthesis**

To assess the effect of the mutations on KDSR enzymatic activity, the six mutations identified in all four patients were introduced into yeast and HEK 293T cells. Two mutant plasmids were designed for the c.417+3A>C variant, one predicting skipping of exon 5 only (Δ5) and the other loss of both exons 5 and 6 (Δ5Δ6). With respect to the c.879G>A variant, the predicted mutant product, Δ10+VSSA, was generated (**Figure 3a**).

A yeast complementation assay was performed using yeast grown on plates with or without phytosphingosine (PHS). Because sphingolipids are essential for cell viability, Δ*tsc10* yeast cells cannot grow normally unless the addition of PHS or dihydrosphingosine (DHS) to the medium bypasses the requirement of *de novo* sphingolipid synthesis. Therefore, under these circumstances, yeast would not be able to grow normally if the *KDSR* mutants impair enzymatic activity. This assay revealed that the mutations (illustrated for Patients 1, 2 and 3; **Figure 3b**) diminished the ability of yeast to grow in the absence of PHS. The p.Phe138Cys mutant had the mildest effect. In comparison, the Δ5, Δ5Δ6, and Δ10+VSSA mutants (representing the c.417+3A>C and c.879G>A mutations) resulted in the most significant impairment of yeast growth (**Figure 3b**).

To assess the enzymatic activity *in vitro*, all the mutant constructs were introduced into HEK 293T cells (**Figure 3c**) and the levels of DHS were quantified. Consistent with the yeast complementation assay, this revealed that most of the mutants led to a significant reduction in DHS synthesis (**Figure 3d**). The only exception was the p.Gly182Ser (c.544G>A)

For Review Only

variant, which showed no significant difference in DHS synthesis compared to wild-type (**Figure 3d**).

These results offer some insight into explaining the discrepancy in phenotypic severity between the patients. One of the two mutations harbored by the clinically milder Patients 1 and 2 (c.413T>G; p.Phe138Cys) results in a mutant protein with ~70% of enzymatic activity compared to wild-type KDSR. In contrast, the mutations identified in the more severely affected Patient 3 (c.812G>A; p.Gly271Glu) and (c.879G>A; Δ10+VSSA) led to mutant products with only ~25% of activity compared to wild-type KDSR. These differences in enzymatic activity thus potentially relate to localized or generalized skin manifestations. For Patient 4, although the activity of the p.Glu75Asnfs*2 (c.223_224delGA) mutant was dramatically reduced (similar to empty vector), the activity of p.Gly182Ser (c.544G>A) was comparable to that of wild-type; this suggests that the latter variant has a distinct functional impact that was not revealed by this assay (see Discussion).

***KDSR* expression and ceramide immunolabeling are reduced in patient skin**

Quantitative PCR (qPCR) was performed using whole skin RNA from Patient 1, Patient 2 and four healthy individuals. *KDSR* expression was found to be reduced in both affected individuals, but not dramatically (70-80% of control; **Figure 4a**). Of note, expression of *FLG*, *CERS3*, *IVL*, *KRT10* and *KRT14* was increased in both patients (**Figure 4b-f**). Immunofluorescence staining was performed on skin sections from Patient 1, Patient 2 and a control individual to examine changes in protein levels or localization. KDSR labeling was not visibly reduced in patient skin (**Supplementary Figure S1** online). Staining with an anti-ceramide antibody revealed reduced (but not absent) ceramide levels in patient skin, supporting the hypothesis that *KDSR* mutations lead to dysregulation of ceramide

For Review Only

biosynthesis. In keeping with the gene expression changes observed, immunoreactivity of CERS3, filaggrin and loricin was increased in both patients (**Supplementary Figure S1** online). Taken together, these alterations suggest that reduction of KDSR activity leads to diminished levels of ceramide in patients. This in turn may lead to a feedback loop causing increased expression of CERS3 and terminal differentiation markers such as keratin 10, involucrin, filaggrin and loricrin.

***KDSR* mutations lead to variable alterations in skin lipids**

The levels of 11 major ceramide species in the skin of the forearm, wrist and palm were assessed by tape stripping and liquid chromatography-mass spectrometry analysis. In the forearms of Patients 1 and 2 (uninvolved skin), there was no significant difference in the total ceramide, ceramide components or average carbon numbers between the affected individuals and their unaffected mothers (**Supplementary Figure S2** online). In contrast, in the affected wrist skin, the levels of total ceramide, CER[EOS], CER[EOH], CER[NP], CER[NH] and CER[NS], were reduced in the patients' samples. Additionally, the average carbon numbers of ceramides indicated that short-chain ceramides, CER[NDS], CER[NS] and CER[AS], were increased in the patients' skin. However, due to the small number of samples, statistical analyses could not be performed. Likewise, in the affected palm skin samples, the levels of total ceramide were decreased in Patient 1 compared to his mother. In contrast, there was no difference in the levels of total or individual ceramides between Patient 2 and his mother. This discrepancy may be explained by the milder phenotype in Patient 2 compared to Patient 1. The average carbon numbers of ceramides showed that short-chain ceramides, CER[NDS], CER[NS], CER[NP], CER[ADS], CER[AS] and CER[AP], were increased both patients' palm. KDSR is one of the key enzymes involved in the *de novo* pathway of

For Review Only

sphingolipid synthesis, acting between serine palmitoyl transferase (SPT) and CERS. Therefore, KDSR deficiency may affect this cascade and lead to a reduction in the levels of synthesis of total and downstream products.

***KDSR* mutations reduce platelet number and function**

Detailed analysis of platelets was performed in Patients 1 and 2, their respective mothers and healthy controls. No morphologic abnormalities in platelets were noted (**Supplementary Figure S3** online) although flow cytometry evaluation of platelet volume was slightly increased in the patients (**Supplementary Table S2** online). The patients' platelets expressed normal levels of adhesive surface glycoproteins, but a lower level of phophatedylserine exposure in terms of basal annexin V binding positive percentages and also reduced thromboplastin expression in unstimulated washed platelets (**Supplementary Table S2** online). Next, we performed platelet function analysis by evaluating granule release and the conformational change of $\alpha_{IIb}\beta_3$ integrin (CD62P and PAC-1, respectively) upon stimulation with different platelet agonists. The increment in double-positive (CD62P and PAC-1) platelets was lower in patients than in heterozygotes and controls, specifically with agonists that are known to activate pathways that are highly dependent on Src family kinases, such as thrombin (PAR1p and PAR4p), collagen (convulxin and collagen related peptide [CRP]), and ADP, but not as evident following arachidonic acid stimulation (**Supplementary Figure S4** online).

The plasma S1P concentration in Patient 1, who presented with more severe clinical bleeding, was decreased by 61% compared to control, while the equivalent measure in Patient 2 was reduced by 45% (**Figure 5a**). The observation that serum S1P levels compared to controls were diminished in both patients by only 45% and 36%, respectively, suggests

For Review Only

that erythrocytes contribute to most of the S1P being released in patient samples during blood clotting (**Figure 5a**). Surface-exposed ceramide in human platelets were investigated with an antibody recognizing C24:0 ceramide levels, the predominant form of ceramide present in human platelets (Chen et al., 2013). This antibody detected an obvious increase in ceramide levels in the plasma membrane of controls and carriers of the c.417+3A>C mutation following platelet activation, whereas the intensity of immunostaining was not changed significantly in affected patients (**Figure 5b**).

DISCUSSION

In this study, we identified biallelic mutations in *KDSR* in patients with defective keratinization and thrombocytopenia, implicating *KDSR* as a further candidate gene for hereditary palmoplantar keratodermas and ichthyosis but also demonstrating that KDSR has an important function in platelet biology. Our data suggest that mutations in *KDSR* impair ceramide biosynthesis pathways and function in skin and platelets.

Previously, data linking *KDSR* to disease have been very limited, aside from a missense variant in the bovine ortholog of *KDSR* that was proposed to cause spinal muscular atrophy (Krebs et al., 2007). Intriguingly, however, a *de novo* deletion of human chromosome 18q has been reported previously in an infant with lethal Harlequin ichthyosis (Stewart et al., 2001): this child's karyotype was 46,XY,del(18)(q21.3). The authors hypothesized that the causative gene may be located at or distal to 18q21.3, and that this deletion may have unveiled this autosomal recessive disorder. Indeed, *KDSR* is located at 18q21.33, and thus we speculate that loss of *KDSR* may have been responsible for this individual's phenotype. The vast majority of cases of Harlequin ichthyosis have bialleleic mutations in the lipid transporter gene, *ABCA12* (Akiyama, 2014) but this previous report

For Review Only

(Stewart et al., 2001), and our current findings in two further subjects with Harlequin ichthyosis, identify *KDSR* as a possible additional candidate gene for non-*ABCA12* Harlequin ichthyosis.

The mutations we identified in *KDSR* are predominantly loss-of-function, the one possible exception being p.Gly182Ser (c.544G>A) which did not appear to alter enzyme activity. We speculate that this variant may instead confer a gain-of-function effect, producing deleterious "mock sphingolipids", similar to what has been observed for missense mutations in *SPTLC1*, encoding a subunit of serine palmitoyl transferase (SPT), in hereditary sensory neuropathy type 1 (Bejaoui et al., 2001; Dawkins et al., 2001; Penno et al., 2010).

Sphingolipids are a family of lipids present in eukaryotes, which are involved in a variety of key physiologic functions in the skin, brain, immune system, and blood vessels (Wegner et al., 2016). Ceramides, one of the classes of sphingoid bases, are vital not only for membrane structure integrity but are also essential for critical signaling processes such as cell cycle arrest, migration, chemotaxis, adhesion, and differentiation (Wegner et al., 2016). Additionally, ceramides are relevant to proliferation, inflammation, apoptosis, and autophagy in the context of stress (Uchida, 2014). There are more than 1,000 ceramide species, of which the majority is present in skin stratum corneum (Kihara, 2016). The major route of ceramide formation is the salvage pathway, which delivers 50-90 % of the ceramide, and uses hydrolysis of sphingomyelin by sphingomyelinase (Linn et al., 2001). Ceramide can be also synthesized *de novo* in the endoplasmic reticulum (Linn et al., 2001). The first step in the *de novo* pathway of ceramide synthesis is catalyzed by serine palmitoyltransferase (SPT), condensing L-serine and a fatty acid (FA) to generate 3-ketodihydrosphingosine (KDS). Subsequently, reduction of 3-KDS by KDSR produces dihydrosphingosine (DHS). DHS is the substrate of ceramide synthases, a group of six enzymes, which bind FAs of varying lengths

For Review Only

to the amide group of DHS, thus giving rise to a variety of dihydroceramides (Levy and Futerman, 2010). Finally, dihydroceramide desaturase creates a double bond between positions 4 and 5, generating ceramide.

A number of inherited skin diseases which involve aberrations in genes important in ceramide synthesis and processing have been described. Among these, mutations in *CERS3* are one cause of autosomal recessive congenital ichthyosis (ARCI), associated with a pronounced reduction in VLC ceramides in the skin (Radner et al., 2013). Similarly, mutations in *ELOVL4*, encoding an enzyme necessary for the production of ULC ceramides in the skin, brain and retina, lead to a recessive disorder characterized by ichthyosis, intellectual disability and spastic quadriplegia (Aldahmesh et al., 2011).

The patients with mutations in *KDSR* also exhibit progressive thrombocytopenia and a moderate functional platelet defect that develops early in life. The most likely explanation for the reduction in platelet count is the diminished S1P synthesis. In thrombopoiesis, both extracellular and intracellular normal levels of this lipid mediator are essential in pro-platelet shedding from megakaryocytes in genetically deficient mice (Zhang et al., 2012; Zhang et al., 2013). Therefore, defects in platelet formation and release in the final stage of thrombopoiesis may contribute to the pathogenesis of thrombocytopenia in the *KDSR* patients. Moreover, the functional defects associated with mutations in *KDSR* could be related not only to the reduced synthesis of S1P, but also ceramide. Previous studies in knockout mice have shown that platelets defective in S1P or ceramide fail to activate normally, and that exogenous ceramide or S1P is able to rescue the phenotype of defective platelet secretion and aggregation (Munzer et al., 2014; Urtz et al., 2015).

The platelet abnormalities in the patients proved difficult to treat with conventional approaches but an alternative strategy might be to use drugs such as fingolimod and related

For Review Only

S1P receptor targeting drugs that act as agonists upon initial binding to S1P receptor. Fingolimod administration causes a rapid increase in platelet numbers in mice (Zhang et al., 2012) suggesting that acute agonistic action of the drug on megakaryocyte S1P receptor-induced platelet release. Thus, it could be possible, in patients with reduced but not absent KDSR enzymatic activity, to therapeutically regulate platelet deficiencies by targeting the S1P receptor. Regarding treatment of the skin, systemic retinoid was only given to one subject (Patient 3). Although there was a reduction in skin scaling thereafter, the onset of sepsis and early demise limited therapeutic evaluation of retinoid therapy.

In conclusion, our data reveal defective ceramide biosynthesis due to loss-of-function mutations in *KDSR* to be responsible for some previously uncharacterized scaly skin disorders (localized or generalized) with accompanying thrombocytopenia. This discovery not only offers new insights into the role of ceramides in skin and platelet biology, but also has implications for patient diagnostics, prognostics and therapeutics.

MATERIALS & METHODS

The full description of all materials and methods used in this study for venous blood sampling for DNA, platelet, plasma and serum studies, as well as methodology for WES, cell culture and transfection, immunofluorescence microscopy, qPCR, and platelet microscopy and flow cytometry are provided in the **Supplementary Materials** online.

Yeast strain and medium

The yeast *Saccharomyces cerevisiae* strain KHY625 (*MAT**a** ura3 his3 trp1 leu2* Δ*tsc10::LEU2*; Kihara and Igarashi, 2004) harboring a *URA3* marker-containing plasmid was grown on synthetic complete minus uracil (SC-URA; 0.67% yeast nitrogen base, 2% D-glucose, 0.5%

For Review Only

casamino acids, 20 mg/L adenine, and 20 mg/L tryptophan) plates with or without 5 μM phytosphingosine (PHS) and 0.0015% Nonidet P-400 (dispersant) at 30 °C.

Plasmid generation

Human *FVT-1*/*KDSR* cDNA was digested from the pAK591 plasmid (Kihara and Igarashi, 2004) and cloned into pCE-puro 3xFLAG-1, the mammalian expression vector designed for N-terminal 3xFLAG-tagged protein production. Four of the identified mutations (F138C, Δ5, Δ5Δ6, and Q271E) were created using the QuikChange Site-Directed Mutagenesis Kit (Agilent Technologies, Santa Clara, CA) and the primers listed in **Supplementary Table S5** online. The Δ10+VSSA and E75Nfs*2 mutants were produced by amplifying the mutated *KDSR* gene using the primers KDSR-F and KDSR Δ10+VSSA-R, and the primers KDSR-F and KDSR E75Nfs*2, respectively (**Supplementary Table S5** online), followed by cloning into the pCE-puro 3xFLAG-1 vector. For expression in yeast, wild type and mutant *KDSR* plasmids were transferred into pAKNF316 (*CEN*, *URA3* marker), the yeast expression vector designed to produce N-terminally 3xFLAG-tagged protein under the control of a glyceraldehyde 3-phosphate dehydrogenase (*GAPDH*) promoter.

Immunoblotting

Immunoblotting was performed as described previously (Kitamura et al., 2015) using anti-FLAG M2 antibody (1.85 μg/mL; Sigma, St. Louis, MO) as the primary antibody and an HRP-conjugated anti-mouse IgG $F(ab')_2$ fragment (diluted 1:7500; GE Healthcare Life Sciences, Piscataway, NJ) as the secondary antibody.

***In vitro* 3-ketodihyrosphingosine (KDS) reductase assay**

For Review Only

Cells were suspended in buffer A [50 mM Tris-HCl (pH 7.5), 10% glycerol, 150 mM NaCl, 1 mM EDTA, 1× protease inhibitor mixture (Complete™ EDTA free; Roche Diagnostics, Basel, Switzerland), 1 mM PMSF, and 1 mM DTT] and lysed by sonication. After ultracentrifugation (100,000 × g, 30 min, 4 °C), the pellet was suspended in buffer A and was used as the total membrane fraction. Protein amounts were quantified using the Pierce BCA Protein Assay Kit (Thermo Fisher Scientific, Waltham, MA). *In vitro* KDS reductase assay was performed by incubating the total membrane fraction (1 µg) with 1 mM NADPH and 10 µM KDS at 37 °C for 1 h. Lipids were extracted by mixing with successive additions of 3.75 volume of chloroform/methanol/HCl (100:200:1, vol/vol/vol), 1.25 volume of chloroform, and 1.25 volume of water. Phases were separated by centrifugation (20,000 × g, room temperature, 3 min). The resulting organic (lower) phase was recovered, dried, and dissolved in methanol. The reaction product dihydrosphingosine (DHS) was detected by ultra performance liquid chromatography (UPLC) coupled with electrospray ionization (ESI) tandem triple quadrupole MS (Xevo TQ-S; Waters, Milford, MA). The UPLC solvent systems and ESI condition were described previously (Yamamoto et al., 2016). DHS was detected by multiple reaction monitoring by selecting the *m/z* value of 302.2 at Q1 and the *m/z* value of 266.0 at Q3 with the collision energy setting at 20 V in positive ion mode. DHS levels were quantified using a standard curve plotted from serial dilutions of DHS (Avanti Polar Lipids, Alabaster, AL) standard. Data were analyzed using MassLynx software (Waters).

Tape stripping for ceramide analysis

To examine the ceramide species present in the stratum corneum, tape stripping was performed by pressing an acryl film tape (456#40, Teraoka Seisakusho, Tokyo, Japan) to the skin of the forearm, wrist and palm. Five strips measuring 25 mm x 50 mm each were

For Review Only

obtained from a single individual. The samples were then subjected to liquid chromatography-mass spectrometry (LC-MS) analysis to assess the levels of 11 major ceramide species (Ishikawa et al., 2013). Samples were taken from two unaffected mothers (Families 1 and 2) as a control.

CONFLICT OF INTEREST

None declared.

ACKNOWLEDGEMENTS

The Centre for Dermatology and Genetic Medicine is supported by a Wellcome Trust Strategic Award (reference 098439/Z/12/Z). The work was supported by the BBSRC, the MRC and the UK National Institute for Health Research (NIHR) comprehensive Biomedical Research Centre (BRC) award to Guy's and St. Thomas' NHS Foundation Trust, in partnership with the King's College London and King's College Hospital NHS Foundation Trust. The Biobank of Andalusia Public Health System (SSPA) provided the samples from normal blood donors.

For Review Only

REFERENCES

Aldahmesh MA, Mohamed JY, Alkuraya HS, Verma IC, Puri RD, Alaiya AA, et al. Recessive mutations in ELOVL4 cause ichthyosis, intellectual disability, and spastic quadriplegia. Am J Hum Genet 2011;89(6):745-50.

Akiyama M. The roles of ABCA12 in epidermal lipid barrier formation and keratinocyte differentiation. Biochim Biophys Acta 2014;1841(3):435-40.

Bejaoui K, Wu C, Scheffler MD, Haan G, Ashby P, Wu L, et al. SPTLC1 is mutated in hereditary sensory neuropathy, type 1. Nat Genet 2001;27(3):261-2.

Chen WF, Lee JJ, Chang CC, Lin KH, Wang SH, Sheu JR. Platelet protease-activated receptor (PAR)4, but not PAR1, associated with neutral sphingomyelinase responsible for thrombin-stimulated ceramide-NF-kappaB signaling in human platelets. Haematologica 2013;98(5):793-801.

Dawkins JL, Hulme DJ, Brahmbhatt SB, Auer-Grumbach M, Nicholson GA. Mutations in SPTLC1, encoding serine palmitoyltransferase, long chain base subunit-1, cause hereditary sensory neuropathy type I. Nat Genet 2001;27(3):309-12.

Fischer J. Autosomal recessive congenital ichthyosis. J Invest Dermatol 2009;129(6):1319-21.

Ishikawa J, Shimotoyodome Y, Ito S, Miyauchi Y, Fujimura T, Kitahara T, et al. Variations in the ceramide profile in different seasons and regions of the body contribute to stratum corneum functions. Arch Dermatol Res 2013;305(2):151-62.

Kihara A. Synthesis and degradation pathways, functions, and pathology of ceramides and epidermal acylceramides. Prog Lipid Res 2016;63:50-69.

Kihara A, Igarashi Y. FVT-1 is a mammalian 3-ketodihydrosphingosine reductase with an active site that faces the cytosolic side of the endoplasmic reticulum membrane. J Biol Chem 2004;279(47):49243-50.

For Review Only

Kitamura T, Takagi S, Naganuma T, Kihara A. Mouse aldehyde dehydrogenase ALDH3B2 is localized to lipid droplets via two C-terminal tryptophan residues and lipid modification. Biochem J 2015;465(1):79-87.

Krebs S, Medugorac I, Rother S, Strasser K, Forster M. A missense mutation in the 3-ketodihydrosphingosine reductase FVT1 as candidate causal mutation for bovine spinal muscular atrophy. Proc Natl Acad Sci U S A 2007;104(16):6746-51.

Levy M, Futerman AH. Mammalian ceramide synthases. IUBMB Life 2010;62(5):347-56.

Linn SC, Kim HS, Keane EM, Andras LM, Wang E, Merrill AH, Jr. Regulation of de novo sphingolipid biosynthesis and the toxic consequences of its disruption. Biochem Soc Trans 2001;29(Pt 6):831-5.

Munzer P, Borst O, Walker B, Schmid E, Feijge MA, Cosemans JM, et al. Acid sphingomyelinase regulates platelet cell membrane scrambling, secretion, and thrombus formation. Arterioscler Thromb Vasc Biol 2014;34(1):61-71.

Oji V, Tadini G, Akiyama M, Blanchet Bardon C, Bodemer C, Bourrat E, et al. Revised nomenclature and classification of inherited ichthyoses: results of the First Ichthyosis Consensus Conference in Soreze 2009. J Am Acad Dermatol 2010;63(4):607-41.

Penno A, Reilly MM, Houlden H, Laura M, Rentsch K, Niederkofler V, et al. Hereditary sensory neuropathy type 1 is caused by the accumulation of two neurotoxic sphingolipids. J Biol Chem 2010;285(15):11178-87.

Radner FP, Marrakchi S, Kirchmeier P, Kim GJ, Ribierre F, Kamoun B, et al. Mutations in CERS3 cause autosomal recessive congenital ichthyosis in humans. PLoS Genet 2013;9(6):e1003536.

Sakiyama T, Kubo A. Hereditary palmoplantar keratoderma "clinical and genetic differential diagnosis". J Dermatol 2016;43(3):264-74.

For Review Only

Stewart H, Smith PT, Gaunt L, Moore L, Tarpey P, Andrew S, et al. De novo deletion of chromosome 18q in a baby with harlequin ichthyosis. Am J Med Genet 2001;102(4):342-5.

Uchida Y. Ceramide signaling in mammalian epidermis. Biochim Biophys Acta 2014;1841(3):453-62.

Urtz N, Gaertner F, von Bruehl ML, Chandraratne S, Rahimi F, Zhang L, et al. Sphingosine 1-Phosphate Produced by Sphingosine Kinase 2 Intrinsically Controls Platelet Aggregation In Vitro and In Vivo. Circ Res 2015;117(4):376-87.

Wegner MS, Schiffmann S, Parnham MJ, Geisslinger G, Grosch S. The enigma of ceramide synthase regulation in mammalian cells. Prog Lipid Res 2016;63:93-119.

Xiong HY, Alipanahi B, Lee LJ, Bretschneider H, Merico D, Yuen RK, et al. RNA splicing. The human splicing code reveals new insights into the genetic determinants of disease. Science 2015;347(6218):1254806.

Yamamoto S, Yako Y, Fujioka Y, Kajita M, Kameyama T, Kon S, et al. A role of the sphingosine-1-phosphate (S1P)-S1P receptor 2 pathway in epithelial defense against cancer (EDAC). Mol Biol Cell 2016;27(3):491-9.

Zhang L, Orban M, Lorenz M, Barocke V, Braun D, Urtz N, et al. A novel role of sphingosine 1-phosphate receptor S1pr1 in mouse thrombopoiesis. J Exp Med 2012;209(12):2165-81.

Zhang L, Urtz N, Gaertner F, Legate KR, Petzold T, Lorenz M, et al. Sphingosine kinase 2 (Sphk2) regulates platelet biogenesis by providing intracellular sphingosine 1-phosphate (S1P). Blood 2013;122(5):791-802.

For Review Only

FIGURE LEGENDS

Figure 1. Pedigrees and mutations identified in *KDSR*. (a-d) Family pedigrees of the four patients with compound heterozygous mutations in *KDSR*. '+' denotes the wild-type allele. (e) Schematic of *KDSR* to show the six compound heterozygous mutations identified in this study.

Figure 2. Clinical features of Patient 1. (a) Diffuse palmar keratoderma. (b) Perianal hyperkeratosis. (c) Bilateral diffuse plantar keratoderma.

Figure 3. Mutations in *KDSR* impair enzymatic activity *in vitro*. (a) Total lysates prepared from KHY625 (*Δtsc10*) cells harboring an empty vector or the plasmid encoding wild-type (WT) or mutant *3xFLAG-KDSR* were separated by SDS-PAGE and subjected to immunoblotting using anti-FLAG M2 antibody. (b) KHY625 cells bearing the indicated plasmid were grown serially diluted at 1:10, spotted on SC-URA plates with or without 5 μM PHS, and grown at 30°C for 3 days. (c and d) HEK 293T cells were transfected with an empty vector or the plasmid encoding WT or mutant *3xFLAG-KDSR*. Twenty-four hours after transfection, total membrane fractions were prepared. (c) Total membrane fractions (5 μg protein) were separated by SDS-PAGE and subjected to immunoblotting using anti-FLAG M2 antibody. (d) Total membrane fractions were incubated with 10 μM KDS and 1 mM NADPH at 37 °C for 1 h. Lipids were extracted and subjected to LC-MS/MS analysis. DHS was detected in the MRM mode and quantified using MassLynx software. Values represent the mean ± SDs of three independent experiments. Statistically significant differences compared to control are indicated. **P*<0.05, ***P*<0.01; *t*-test.

For Review Only

Figure 4. *KDSR* mutations slightly reduce *KDSR* expression but upregulate expression of skin differentiation markers. The mRNA levels of (a) *KDSR*, (b) *FLG*, (c) *KRT10*, (d) *KRT14*, (e) *CERS3*, and (f) *IVL* were evaluated by q-PCR in skin from Patients 1 and 2 and four healthy controls. *18S* was used to normalize gene expression levels.

Figure 5. *KDSR* mutations reduce sphingosine 1 phosphate (S1P) and ceramide expression in plasma, serum and activated platelets. (a) S1P concentration in blood plasma and serum samples obtained from Patients 1 and 2, and normal subjects. Red bars represent the affected individuals, and green bars two parallel controls. (b) Ceramide expression in stimulated platelets in response to 250 mM PAR1p. Bars colored in lighter shades of red, blue, and green represent unstimulated cells and the bars in darker shades of each respective color indicate activated platelets. The values shown are the means of (a) S1P concentration and (b) median fluorescence intensity (MFI). The error bars indicate the SEM.

For Review Only

TABLES

Patient	Country of origin	Dermatologic phenotype	Thrombocytopenia	Mutations in *KDSR* & amino acid change	1000 Genomes Project frequency	ExAC frequency	SIFT (score)	PolyPhen-2 (score)	Mutation Taster
1	Spain	Palmoplantar and perianal keratoderma	+	c.413T>G: p.Phe138Cys	0	8.3×10^{-5}	Damaging	Probably damaging	Disease-causing
				c.417+3A>C	0	0	N/A	N/A	Disease-causing
2	Spain	Palmoplantar and perianal keratoderma	+	c.413T>G: p.Phe138Cys	0	8.3×10^{-5}	Damaging	Probably damaging	Disease-causing
				c.417+3A>C	0	0	N/A	N/A	Disease-causing
3	United Kingdom	Harlequin ichthyosis	+	c.812G>A: p.Gly271Glu	0	0	Damaging	Probably damaging	Disease-causing
				c.879G>A: p.Gln293Gln	0	3.3×10^{-5}	N/A	N/A	Disease-causing
4	Japan	Harlequin ichthyosis	+	c.223_224delGA: p.Glu75Asnfs*2	0	0	N/A	N/A	Disease-causing
				c.544G>A: p.Gly182Ser	0	8.2×10^{-6}	Damaging	Probably damaging	Disease-causing

Table 1. Summary of clinical and mutation details of all four affected individuals.

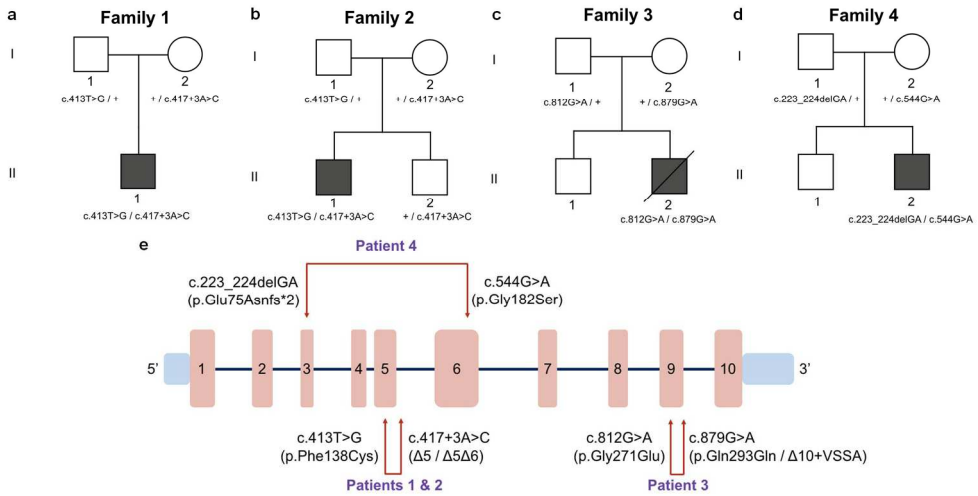

Figure 1. Pedigrees and mutations identified in KDSR. (a-d) Family pedigrees of the four patients with compound heterozygous mutations in KDSR. '+' denotes the wild-type allele. (e) Schematic of KDSR to show the six compound heterozygous mutations identified in this study.

400x200mm (300 x 300 DPI)

view Only

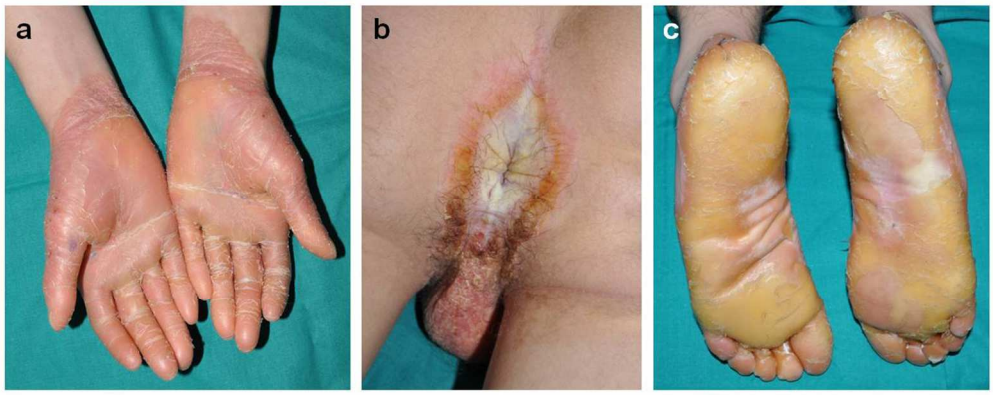

Figure 2. Clinical features of Patient 1. (a) Diffuse palmar keratoderma. (b) Perianal hyperkeratosis. (c) Bilateral diffuse plantar keratoderma.

230x92mm (300 x 300 DPI)

Review Only

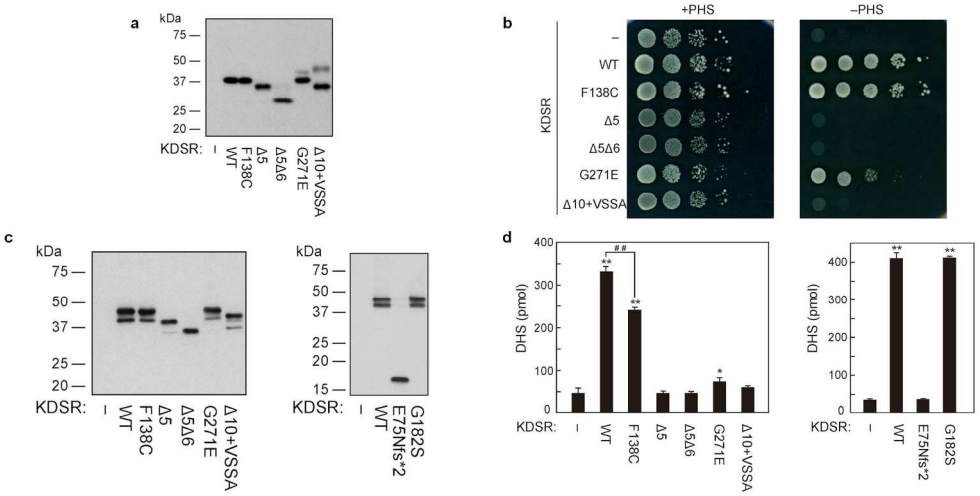

Figure 3. Mutations in KDSR impair enzymatic activity in vitro. (a) Total lysates prepared from KHY625 (Δtsc10) cells harboring an empty vector or the plasmid encoding wild-type (WT) or mutant 3xFLAG-KDSR were separated by SDS-PAGE and subjected to immunoblotting using anti-FLAG M2 antibody. (b) KHY625 cells bearing the indicated plasmid were grown serially diluted at 1:10, spotted on SC-URA plates with or without 5 μM PHS, and grown at 30°C for 3 days. (c and d) HEK 293T cells were transfected with an empty vector or the plasmid encoding WT or mutant 3xFLAG-KDSR. Twenty-four hours after transfection, total membrane fractions were prepared. (c) Total membrane fractions (5 μg protein) were separated by SDS-PAGE and subjected to immunoblotting using anti-FLAG M2 antibody. (d) Total membrane fractions were incubated with 10 μM KDS and 1 mM NADPH at 37 °C for 1 h. Lipids were extracted and subjected to LC-MS/MS analysis. DHS was detected in the MRM mode and quantified using MassLynx software. Values represent the mean ± SDs of three independent experiments. Statistically significant differences compared to control are indicated. *P<0.05, **P<0.01; t-test.

401x200mm (300 x 300 DPI)

Only

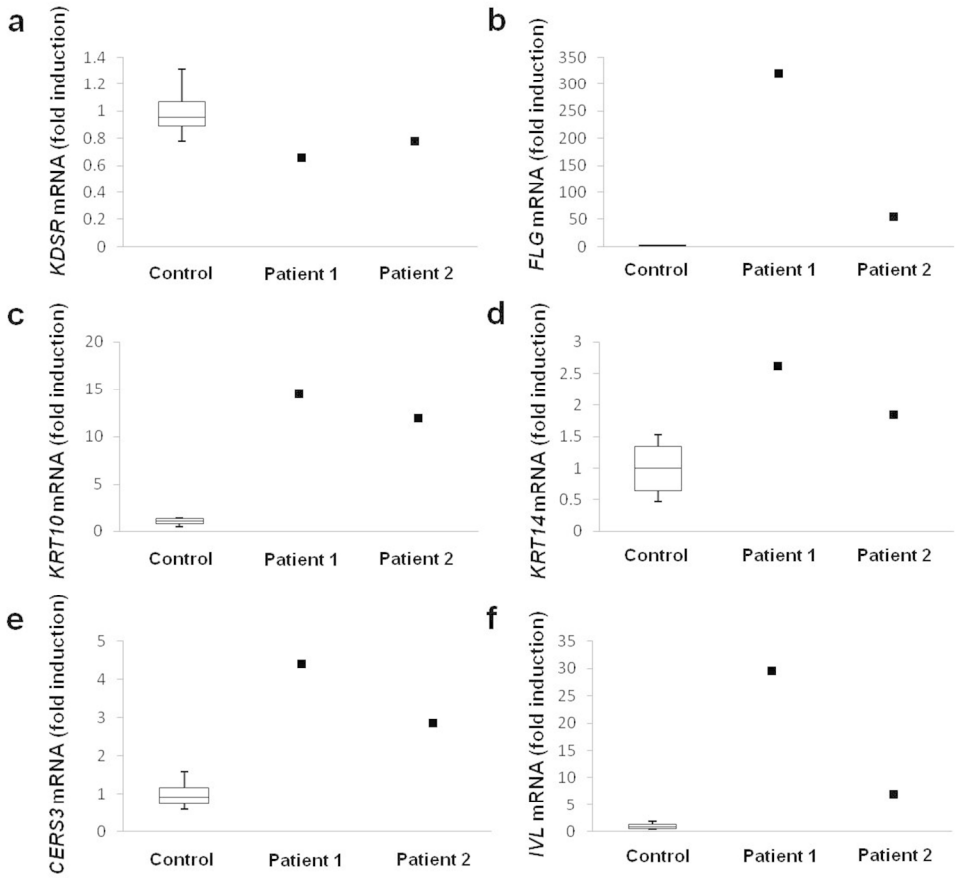

Figure 4. KDSR mutations slightly reduce KDSR expression but upregulate expression of skin differentiation markers. The mRNA levels of (a) KDSR, (b) FLG, (c) KRT10, (d) KRT14, (e) CERS3, and (f) IVL were evaluated by q-PCR in skin from Patients 1 and 2 and four healthy controls. 18S was used to normalize the gene expression levels.

196x182mm (300 x 300 DPI)

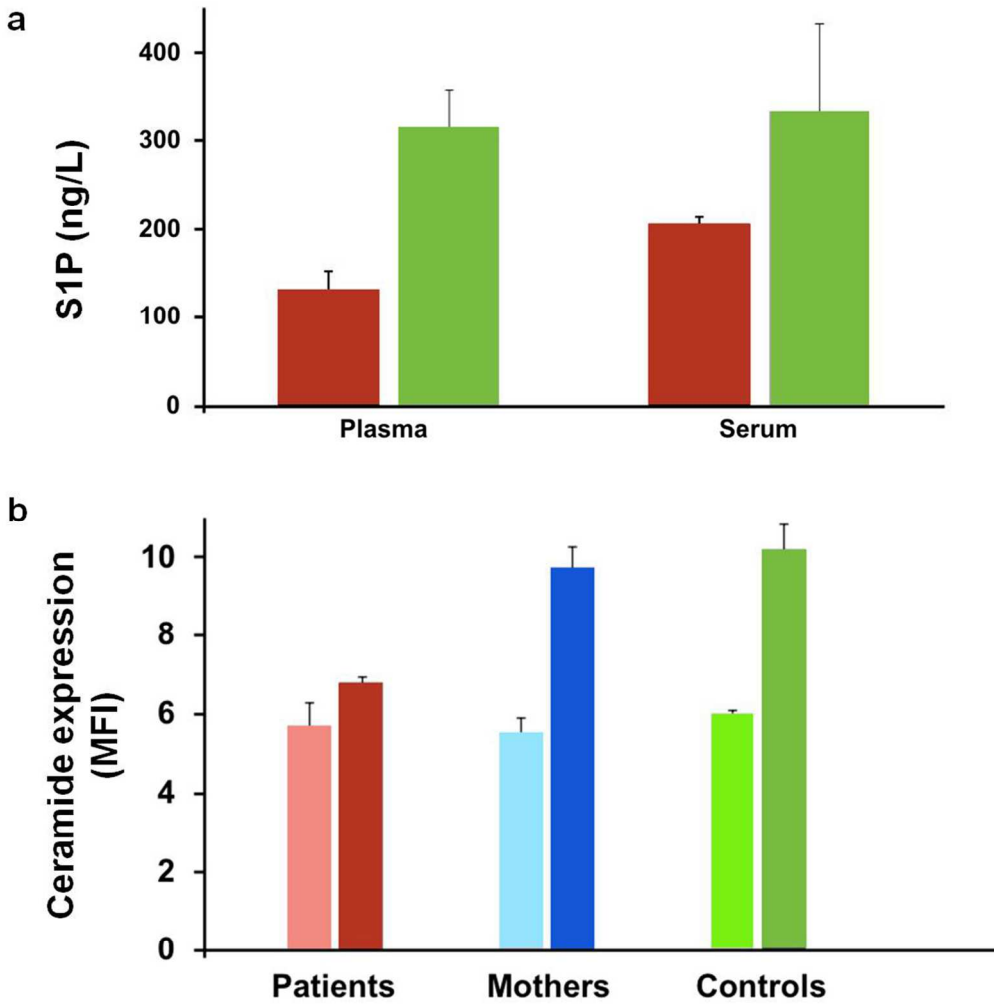

Figure 5. KDSR mutations reduce sphingosine 1 phosphate (S1P) and ceramide expression in plasma, serum, and activated platelets. (a) S1P concentration in blood plasma and serum samples obtained from Patients 1 and 2, and normal subjects. Red bars represent the affected individuals, and green bars two parallel controls. (b) Ceramide expression in stimulated platelets in response to 250 mM PAR1p. Bars colored in lighter shades of red, blue, and green represent unstimulated cells and the bars in darker shades of each respective color indicate activated platelets. The values shown are the means of (a) S1P concentration and (b) median fluorescence intensity (MFI). The error bars indicate the SEM.

193x202mm (300 x 300 DPI)

Supplementary Materials and Methods

Ethics statement

This study was conducted in compliance with the Declaration of Helsinki and all participants provided informed consent. This study was also approved by the relevant institutional authorities, namely the St Thomas' Hospital Ethics Committee, UK ("Molecular basis of inherited skin diseases" 07/H0802/104), the Bioethics Committee of the Nagoya University Graduate School of Medicine, Japan, and the Ethics Committee of Hospital Universitario Reina Sofía, Murcia, Spain.

Blood sampling

Venous blood was drawn from affected individuals, their mothers, and two parallel healthy controls into 7.5% K3 EDTA tubes (for blood counts and DNA isolation), buffered 0.105 M sodium citrate (for platelet function studies), or in empty tubes (for preparation of serum) using a 20-gauge needle. Samples were maintained at room temperature until processing. Platelet-rich plasma (PRP) and platelet-poor plasma (PPP) were separated from blood samples by stepwise centrifugations at 140 x g for 10 min and then 1200 x g for 20 min at room temperature (RT). Serum was obtained from non-anticoagulated blood by incubation at 37°C for 30 min followed by centrifugation (1200 x g, 20 min). PPP and serum aliquots were stored frozen at -80°C until used in the human sphingosine 1 phosphate enzyme-linked immunosorbent assay (Shanghai Crystal Day Biotech Co., LTD, Shanghai, China). For some studies, washed platelets resuspended in Tyrode´s buffer (Guerrero et al., 2005) were used.

For Review Only

Whole-exome sequencing

Genomic DNA was extracted and whole-exome capture was performed by in-solution hybridization (Agilent All Exon V4 kit, Agilent Technologies, Santa Clara, CA, USA). Massively parallel sequencing was performed with the Illumina HiSeq 2000 platform with 100-bp paired-end reads (San Diego, CA). The reads produced were aligned to the reference human genome using the NovoAlign software package (Novocraft Technologies Sdn Bhd, Selangor, Malaysia). Reads mapping to multiple regions and duplicate reads (arising from PCR clonality or optical duplicates) were excluded from downstream analyses.

Cell culture and transfection

HEK 293T cells were grown in Dulbecco's Modified Eagle's Medium (D6429; Sigma, St. Louis, MO) supplemented with 10% FBS, 100 U/mL penicillin, and 100 µg/mL streptomycin in a 5% CO_2 incubator at 37 °C. Dishes were pre-coated with 0.1 mg/mL collagen (Cellmatrix type I-P, Nitta Gelatin, Osaka, Japan). Transfections were conducted using Lipofectamine Plus™ Reagent (Thermo Fisher Scientific, Waltham, MA), according to the manufacturer's instructions.

Immunofluorescence microscopy

Following informed consent, skin samples were taken from patients and healthy controls under local anesthetic. Samples were placed in Michel's medium at room temperature during transportation. Skin samples were washed in 0.1 M Dulbecco's Phosphate Buffered

For Review Only

Saline (PBS) for 1 hour at 4 °C, mounted in Optimal Cutting Temperature compound (Agar Scientific, Stansted, UK) and immediately frozen in liquid nitrogen cooled n-heptane. Cryostat sections of 5 µm were cut and transferred onto Superfrost™ Plus slides (Thermo Scientific, UK). The samples were air dried and stored in a -20 °C freezer until required. Prior to staining, slides were air dried for 10 minutes, immersed in PBS for 5 minutes and incubated with goat/rabbit serum (Sigma-Aldrich) for 2 minutes at room temperature. Primary antibodies were diluted in 1% bovine serum albumin (BSA) (Sigma-Aldrich, Gillingham, Dorset, UK) in PBS at the desired concentration (see **Supplementary Table S3** for the list of primary antibodies used). A negative control was prepared with serum without adding any primary antibody. The slides were then incubated with the primary antibody or negative control solution for 1 hour at 37 °C or overnight at 4 °C in a humidified chamber. They were then washed twice in PBS for 10 minutes and incubated with the relevant fluorescein-conjugated secondary antibodies (Vector Labs, CA) diluted 1:500 in 1% BSA/PBS for 1 hour at room temperature in a dark humidified air chamber. The samples were washed twice in PBS for 10 minutes and then twice in distilled water for 10 minutes before being mounted in glycerol/PBS-containing vector shield with DAPI (Vector Labs). Images of the slides were captured with a Nikon Eclipse E600 epifluorescence microscope fitted with a Jenoptik CF Cool digital camera (Jenoptik, Jena, Germany).

Quantitative reverse transcription polymerase chain reaction (qPCR)

A 20 µL reaction mixture was made up of 2 µL of cDNA template, 10 µL of Taqman® Mastermix (Thermo Fisher Scientific, UK), 1 µL of gene expression assay (Thermo Fisher Scientific, Paisley, UK) and 7 µL of diethyl pyrocarbonate (DEPC)-treated water (see

For Review Only

Supplementary Table S4 for the list of probes used). Each reaction was performed in triplicate to correct for pipetting errors. The mixture was then pipetted into a MicroAmp Optical 96-well plate (Applied Biosystems) and placed into the ABI 7900HT Fast Real-Time PCR System (Applied Biosystems, Carlsbad, CA). The samples were heated to 50 °C and then 95 °C for 10 minutes for AmpliTaq Gold DNA polymerase activation, followed by 40 cycles at 95 °C for 15 seconds and 60 °C for 1 minute for denaturation, annealing, and elongation. A water sample was included as a no template control to exclude contamination. The mean C_T value for each assay was determined and all experiments were repeated on three independent occasions to enable statistical analyses and correct for experimental viability.

Population genetic analysis

Blood samples were obtained from 43 healthy blood donors from the same region in Spain as Patients 1 and 2, as well as from 49 patients attending the local health center for routine blood sampling due to unrelated conditions. All subjects gave written informed consent to participate in this study, which complied with the Helsinki Declaration and was formally approved by the Ethics Committee of Hospital Universitario Reina Sofía, Murcia, Spain. Genomic DNA from EDTA blood samples was isolated using a DNeasy blood and tissue kit, following the manufacturer's protocol (Qiagen, Hilden, Germany). DNA concentration was measured using a Qubit 2.0 fluorometer (Life Technologies, Carlsbad, CA). Exons 4 and 5 of *KDSR* (NG_028249.1; ENSG00000119537) were screened for mutations using genomic DNA. A 458-bp PCR product was amplified using a primer pair (sense: 5'-GCATATCAGTTGATGTATCTCAAG-3'; antisense: 5'-CCATGGACATCTGAATGCAT-3') that included the c.413T>G and c.417+3A>C mutations, along with two SNPs (rs1809319 and

For Review Only

rs72946535). DNA samples of the 10 individuals carrying the c.413T>G or c.417+3A>C mutations were tested by allele-specific PCR for *linkage* analysis with the specific SNPs. PCR products were sequenced using the ABI 3130xl Genetic Analyzer (Applied Biosystems).

Electron microscopy of platelets

Platelet-rich plasma samples were fixed in 1.25% glutaraldehyde, washed and post fixed in 1% osmic acid containing 1.5% potassium ferrocyanide, dehydrated using graded alcohols and propylene oxide and embedded in Epon as described previously (Navarro-Nunez et al., 2011). Embedded samples were sectioned, stained, and visualized using a Philips Tecnai 12 transmission electron microscope and a Megaview III camera (FEI, Hillsboro, OR).

Flow cytometry for platelets

Platelet expression of major platelet membrane glycoproteins (GP) (GPIa [CD49b], GPIbα [CD42b], CD42a [GPIX], integrin β3 [CD61]), was assessed by flow cytometry in PRP through a direct standard technique with appropriate labeled monoclonal antibodies (Becton Dickinson, San Jose, CA). For analysis of surface-expressed P-selectin (marker of alpha granule release) and binding of PAC-1 (marker for activated αIIbβ3), diluted PRP (~$30x10^9$/L platelets) was stimulated under static conditions (30 min at room temperature) with the desired agonist concentration in the presence of both anti-CD62-PE and PAC1-FITC antibodies (Becton Dickinson). Tissue factor expression (binding of anti-CD142 antibody, Becton Dickinson) and detection of phosphatidylserine using fluorescein labelled Annexin V (Becton Dickinson) was analyzed in unstimulated, washed platelets. To analyze for ceramide

For Review Only

expression in washed platelets, cells were incubated with or without 100 µM PAR1 peptide [PAR1p] and an antibody recognizing C-16 and C-24 ceramide (LifeSpan BioScience, Seattle City, WA). Platelets were washed and incubated with a FITC-conjugated anti-mouse IgM (LifeSpan BioScience). Samples were then run in the FACSCalibur flow cytometer (Becton Dickinson) and the percentage or median fluorescence intensity (MFI) or percentage of positively stained cells was analyzed using the CellQuest software (Becton Dickinson).

For Review Only

References for Supplementary Methods

Guerrero JA, Lozano ML, Castillo J, Benavente-Garcia O, Vicente V, Rivera J. Flavonoids inhibit platelet function through binding to the thromboxane A2 receptor. J Thromb Haemost 2005;3(2):369-76.

Navarro-Nunez L, Teruel R, Anton AI, Nurden P, Martinez-Martinez I, Lozano ML, et al. Rare homozygous status of P43 beta1-tubulin polymorphism causes alterations in platelet ultrastructure. Thromb Haemost 2011;105(5):855-63.

Supplementary Figures

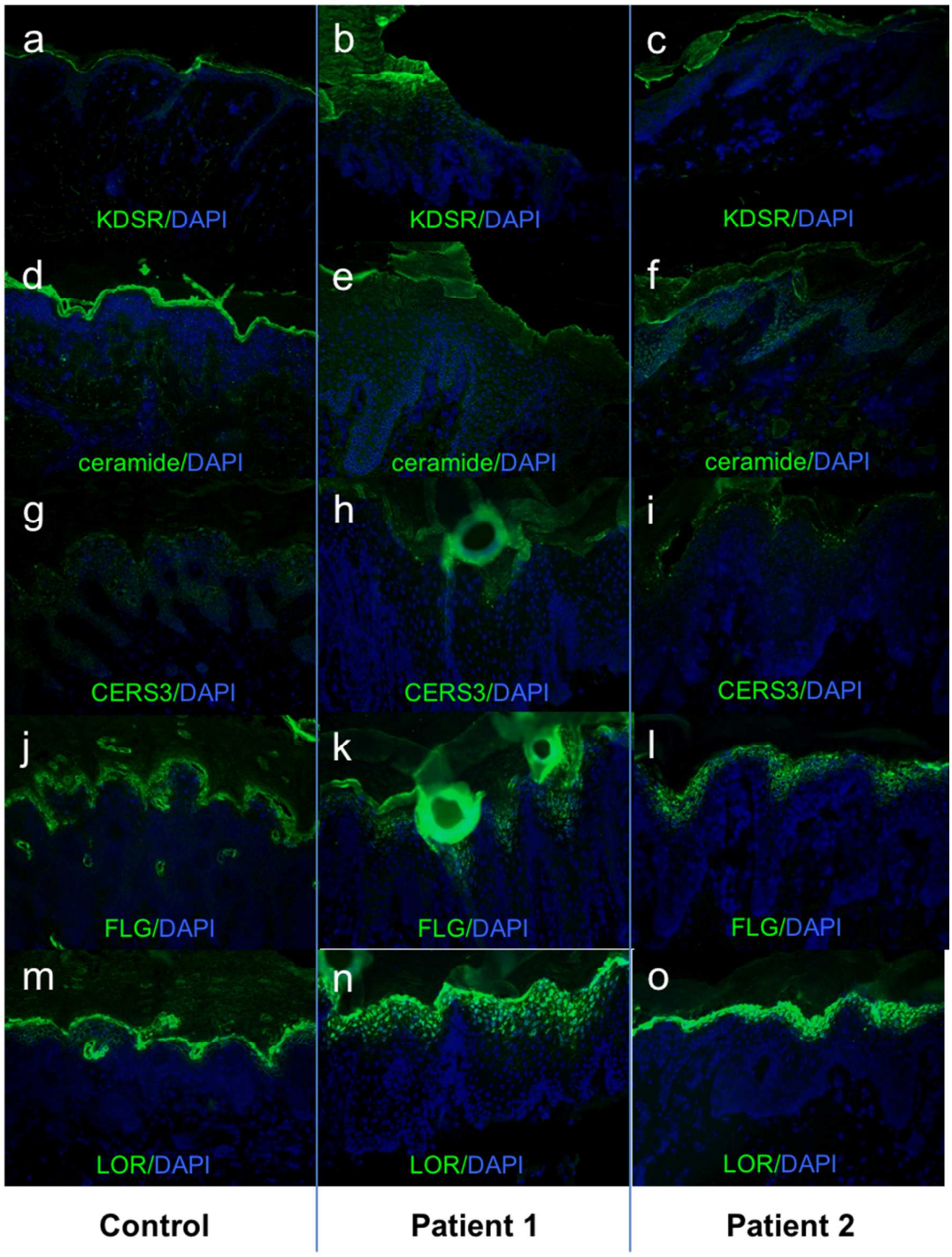

Figure S1. Immunofluorescence analysis in skin from affected patients and control. Immunofluorescence staining reveals reduced ceramide labeling with precocious staining for markers of epidermal differentiation compared to control skin.

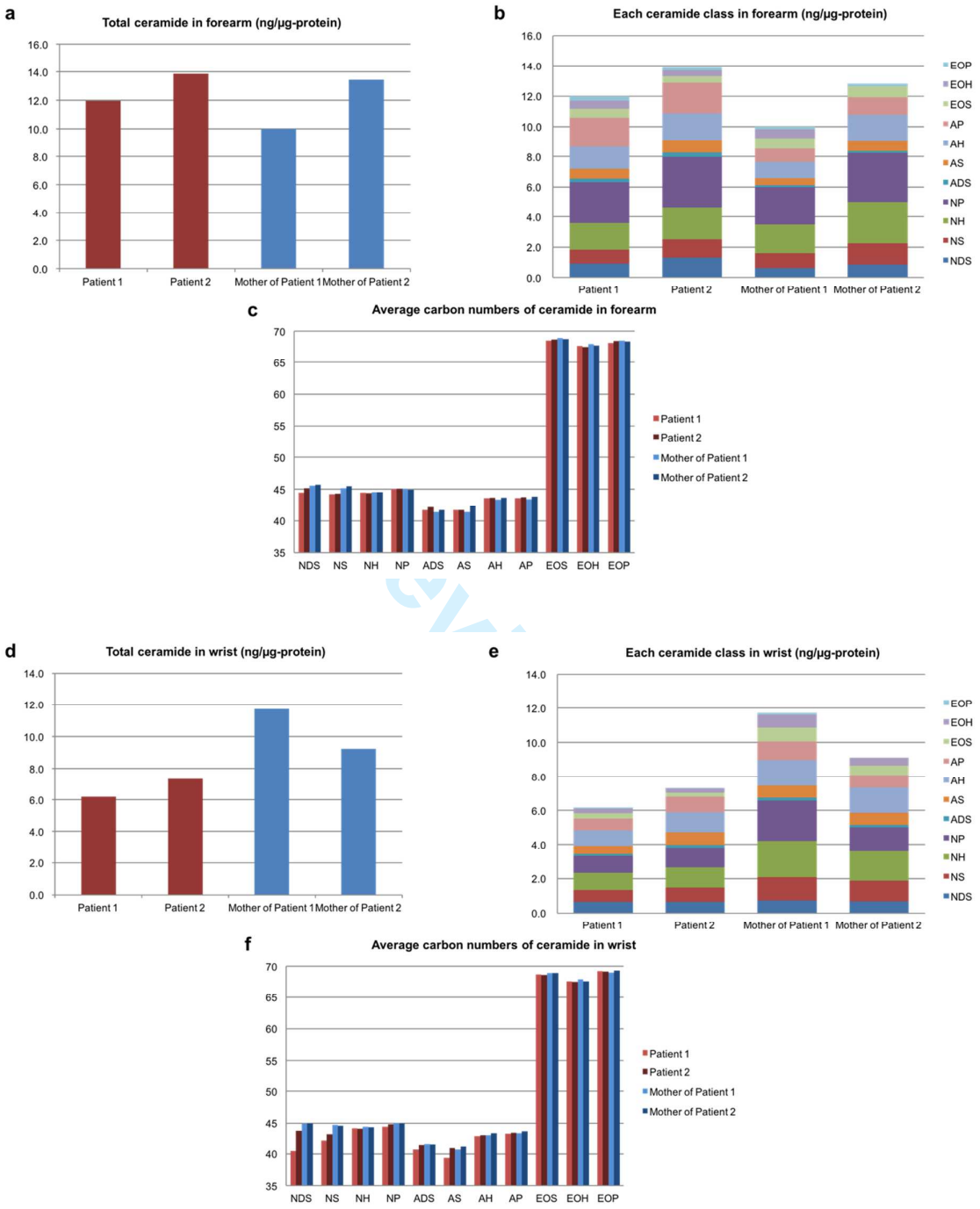
a
Total ceramide in forearm (ng/μg-protein)
16.0
14.0
12.0
10.0
8.0
6.0
4.0
2.0
0.0
Patient 1
Patient 2
Mother of Patient 1
Mother of Patient 2
b
Each ceramide class in forearm (ng/μg-protein)
EOP
EOH
EOS
AP
AH
AS
ADS
NP
NH
NS
NDS
c
Average carbon numbers of ceramide in forearm
70
65
60
55
50
45
40
35
NDS NS NH NP ADS AS AH AP EOS EOH EOP
d
Total ceramide in wrist (ng/μg-protein)
e
Each ceramide class in wrist (ng/μg-protein)
f
Average carbon numbers of ceramide in wrist

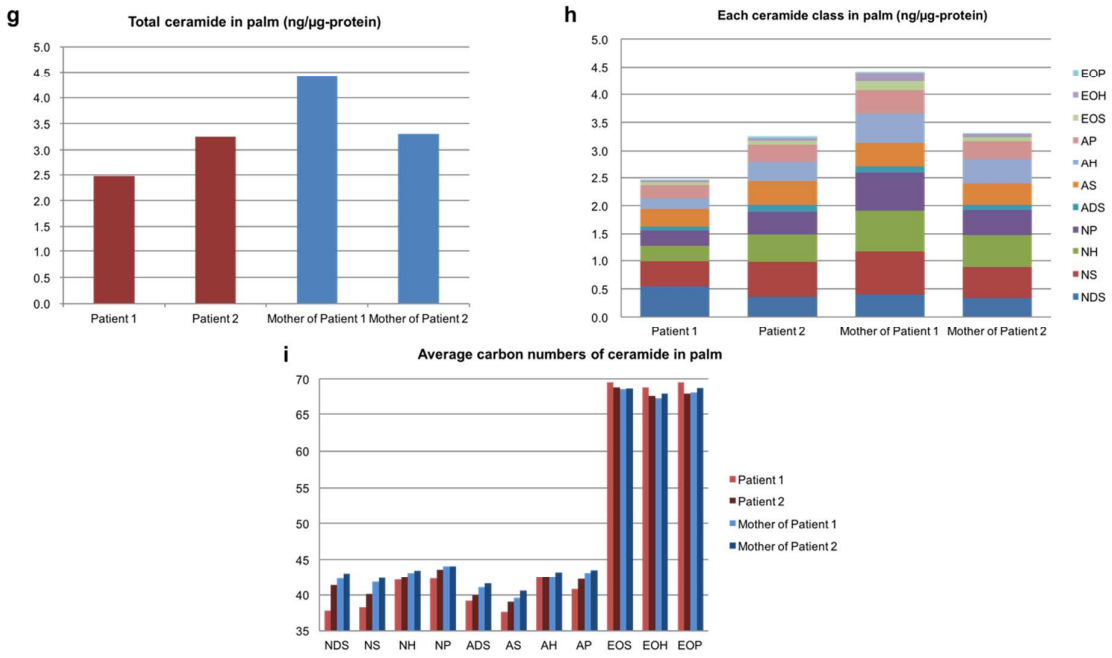

Figure S2. Liquid chromatography-mass spectrometry analysis of total ceramides (CERs) and 11 CER subclasses in the (a-c) forearms, (d-f) wrists, and (g-i) palms of Patients 1 and 2 and their respective mothers.

Accompanying discussion for Figure S2

Ceramides in the skin are integral to skin barrier function. On the one hand, during the process of cornification, the lipid bilayer of the plasma membrane is replaced by a monolayer of acylceramides known as the corneocyte lipid envelope (CLE). These acylceramides bind to proteins of the cornified envelope (Candi et al., 2005; Elias et al., 2014). On the other hand, ceramides account for the 50 % of the lipid lamellae components in the stratum corneum (Breiden and Sandhoff, 2014). Ceramide synthases (CerS) use acyl-CoAs as FA donors, but different CerS have affinities for different length FAs and different tissue distributions (Kihara, 2016). Of these, Cers3 is mainly found in the skin (keratinocytes) and testis, and has a broad specificity for substrate, with affinity toward C18-CoAs (C18

Review Only

ceramide) and longer (Mizutani et al., 2006; Sassa et al., 2016). This enables CerS3 to produce a wide range of ceramides, especially the very long chain (VLC) FA ceramides (C22 ceramides and longer) and the ultra long chain (ULC) FA ceramides (C26 ceramides and longer) (Kihara, 2016). The ULCFA ceramides are prominent in the epidermis, and are often ω-hydroxylated and esterified with linoleic acid, to generate acylceramides, which are most important for the skin barrier function in the stratum corneum (Kihara, 2016). The generation of very long chain FAs in ceramides can also be accomplished by the action of elongation cycles, with the involvement of highly conserved enzymes named elongases (Kihara, 2012). Elongases 1 and 4 (ELOVL1, ELOVL4) are present in the skin, and ELOVL1 is regulated by CerS3 in the stratum granulosum, enabling ELOVL1 to produce C26-CoAs from C24-CoAs (Sassa et al., 2013), which are then elongated to ≥C28-CoAs by ELOVL4 (Okuda et al., 2010).

References

Breiden B, Sandhoff K. The role of sphingolipid metabolism in cutaneous permeability barrier formation. Biochim Biophys Acta 2014;1841(3):441-52.

Candi E, Schmidt R, Melino G. The cornified envelope: a model of cell death in the skin. Nat Rev Mol Cell Biol 2005;6(4):328-40.

Elias PM, Gruber R, Crumrine D, Menon G, Williams ML, Wakefield JS, et al. Formation and functions of the corneocyte lipid envelope (CLE). Biochim Biophys Acta 2014;1841(3):314-8.

Kihara A. Very long-chain fatty acids: elongation, physiology and related disorders. J Biochem 2012;152(5):387-95.

For Review Only

Kihara A. Synthesis and degradation pathways, functions, and pathology of ceramides and epidermal acylceramides. Prog Lipid Res 2016;63:50-69.

Mizutani Y, Kihara A, Igarashi Y. LASS3 (longevity assurance homologue 3) is a mainly testis-specific (dihydro)ceramide synthase with relatively broad substrate specificity. Biochem J 2006;398(3):531-8.

Okuda A, Naganuma T, Ohno Y, Abe K, Yamagata M, Igarashi Y, et al. Hetero-oligomeric interactions of an ELOVL4 mutant protein: implications in the molecular mechanism of Stargardt-3 macular dystrophy. Mol Vis 2010;16:2438-45.

Sassa T, Hirayama T, Kihara A. Enzyme Activities of the Ceramide Synthases CERS2-6 Are Regulated by Phosphorylation in the C-terminal Region. J Biol Chem 2016;291(14):7477-87.

Sassa T, Ohno Y, Suzuki S, Nomura T, Nishioka C, Kashiwagi T, et al. Impaired epidermal permeability barrier in mice lacking elovl1, the gene responsible for very-long-chain fatty acid production. Mol Cell Biol 2013;33(14):2787-96.

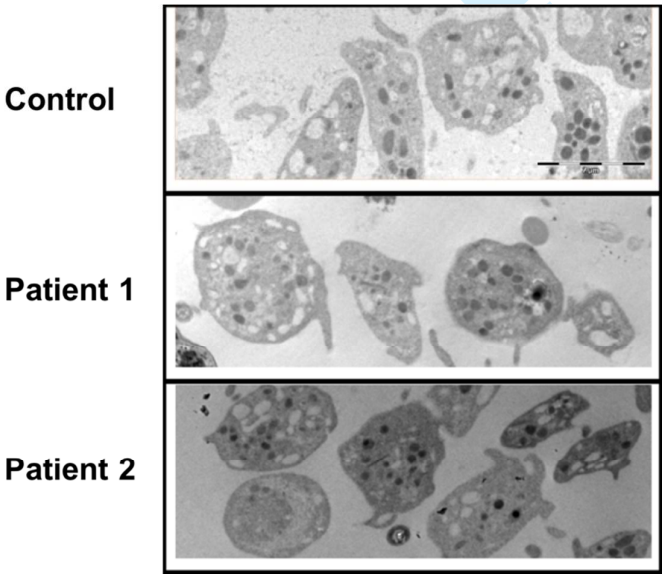

For Review Only

Figure S3. Electron microscopy evaluation of platelets from patients with *KDSR* mutations reveals no major ultrastructural differences compared to control platelets. Platelets were processed for analysis by electron microscopy, as described in the Supplementary Methods. All images are magnified 5800x.

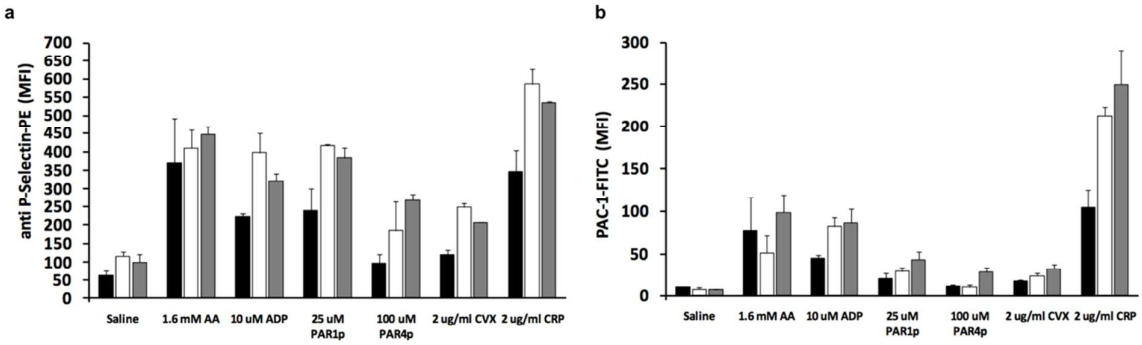

Figure S4. Analysis of platelet function in Patients 1 and 2, their mothers, and normal controls. (a and b) Platelets from compound heterozygotes of the mutations c.413T>G and c.417+3A>C in *KDSR*, their heterozygous mothers (carrying the c.417+3A>C mutation), and healthy unrelated controls (combined data from two subjects), were stimulated under static conditions (30 min at RT) with agonist (1.6 mM Arachidonic acid, 10 µM ADP, 25 µM PAR1 peptide [PAR1p], 100 µM PAR4 peptide [PAR4p], 2 µg/mL convulxin [Cvx], and 2 µg/mL collagen-related-peptide [CRP] in the presence of both PAC-1-FITC and anti-CD62P-PE monoclonal antibodies. The samples were evaluated by flow cytometry and the median fluorescence intensity [MFI]) for alpha granule release (anti-CD62P-PE, panel A) and $\alpha_{IIb}\beta_3$ integrin activation (anti PAC-1-FITC, panel B) is shown. Values presented are the mean of median fluorescence intensity (MFI) ± standard error of mean (SEM) from the two

View Only

compound heterozygote patients (black bars), their mothers (white bars) and two parallel controls (gray bars).

Supplementary Tables

	rs1809319 A/G	rs72946535 G/A	c.413 T>G	c.417+3 A>C
Family 1				
• Patient	**AG**	**GA**	**TG**	**AC**
• Mother	AG	**GA**	TT	**AC**
• Father	**AG**	GG	**TG**	AA
• Brother	AA	**GA**	TT	**AC**
Family 2				
• Patient	**AG**	**GA**	**TG**	**AC**
• Mother	AA	**GA**	TT	**AC**
• Father	**AG**	GG	**TG**	AA
Controls				
• Control 1	**AG**	AA	**TG**	AA
• Control 2	AA	**GA**	TT	**AC**
• Control 3	AG	**GA**	TT	**AC**
Controls (n=92)				
Allele frequencies	0.337	0.071		

Table S1. Population genetic analysis of the *KDSR* mutations identified in Patients 1 and 2. Polymorphisms and mutations in *KDSR* in the two patients, their relatives, and in three control individuals who harbor the disease-causing mutations, as well as the minor allele frequencies of the two polymorphisms in the cohort of controls.

Accompanying text for Table S1

Mutation analysis was performed on samples from the two patients from Spain, their relatives, and controls from the same geographical region for the presence of the identified disease-causing mutations in *KDSR* (c.413T>G and c.417+3A>C). In addition, these samples were tested for the presence of two polymorphisms located within intron 4 of *KDSR*, in an

For Review Only

attempt to elucidate the presence of a potential founder effect, which could explain the identification of identical compound heterozygous mutations in families 1 and 2.

The frequencies of these disease-causing mutations and of the two polymorphisms in 92 control subjects are shown in **Table S1** above. One control individual was heterozygous for the c.413T>G mutation, and two control individuals were heterozygous for the c.417+3A>C variant. The overall carrier frequency of these two mutations in this geographical area was therefore estimated as 1:92 and 1:46, respectively. These figures would therefore lead to a disease incidence of approximately 1 in 17,000 live births. The control cohort also exhibited a lower frequency of the common rs1809319 (A allele 0.337 vs. reported MAF of 0.42), while the rare rs72946535 was overrepresented in the control group (A allele 0.071 vs. reported MAF of 0.01). Allele-specific PCR revealed that in patients, relatives, and controls, the c.413T>G mutation was found only with the G variant of rs1809319, while the c.417+3A>C mutation was present only in association with the A variant of rs72946535 inferring that these variants are tightly linked, and that individuals carrying each of these mutations share a common ancestor.

	P1	P2	Mother of P1	Mother of P2	Control 1	Control 2
WBC (x10^9/L)	16.1	8.2	5.2	8.6	7.2	7.8
Hb (g/dL)	13.9	12.7	12.4	13.5	12.8	14.3
Ht (%)	40.2	37.9	36.6	39.9	37.7	42.6
Platelets (x10^9/L)	24	7	213	226	207	206
FSC (MFI)	32.9	32.9	26.8	27.9	25.7	25.6
CD42b (MFI)	127.2	122.8	152.7	186.2	161.3	199.5
CD42a (MFI)	187.2	189.2	188.1	207.7	180.6	212.8
CD61 (MFI)	209.8	215.3	194.5	237.8	216.7	226.4
CD49b (MFI)	29.5	28.5	33.6	41.1	39.5	31.6

For Review Only

Annexin V (% positive)	2.5	1.7	5.9	4.2	4.7	3.6
Tissue factor (% positive)	4.2	4.4	7.8	5.9	7.5	6.2

Table S2. Blood parameters, platelet size, glycoprotein expression, and annexin V and tissue factor binding in Patients 1 and 2, their mothers, and normal controls. WBC: white blood cells; RBC: red blood cells; Hb: hemoglobin; Ht: hematocrit; FSC: Forward side scatter. P1: Patient 1; P2: Patient 2.

Antigen	Product ID	Source
KDSR	bs-13233R	Bioss Inc, Woburn, MA
CERS3	HPA006092	Sigma-Aldrich, St Louis, MO
FLG	SPM181	Abcam, Cambridge, UK
LOR	ab24722	Abcam, Cambridge, UK
Ceramide	MAB_0011	Glycobiotech, Kukels, Germany
DAPI	H-1200	Vector Labs, Burlingame, CA

Table S3. List of primary antibodies used in skin immunofluorescence studies.

Gene	Assay ID
KDSR	Hs00179997_m1
FLG	Hs00856927_g1
CERS3	Hs00698859_m1
IVL	Hs00846307_s1

For Review Only

KRT10	Hs00166289_m1
KRT14	Hs00265033_m1
18S	Hs03003631_g1

Table S4. List of qPCR probes used in this study. All probes were purchased from Thermo Fisher Scientific, Paisley, UK.

Primer	**DNA sequence**
KDSR F138C-F	5'-CTTGAAGTTAGTACCTGTGAAAGGTTAATGAG-3'
KDSR F138C-R	5'-CTCATTAACCTTTCACAGGTACTAACTTCAAG-3'
KDSR Δ5-F	5'-GTAGAGAATGTCATAAAACAAAGGTTAATGAGCATCAATTAC-3'
KDSR Δ5-R	5'-GTAATTGATGCTCATTAACCTTTGTTTTATGACATTCTCTAC-3'
KDSR Δ5Δ6-F	5'-GTAGAGAATGTCATAAAACAAGTGAAGCCATATAATGTCTAC-3'
KDSR Δ5Δ6-R	5'-GTAGACATTATATGGCTTCACTTGTTTTATGACATTCTCTAC-3'
KDSR G271E-F	5'-CCCTTGGCTCAGATGAGTACATGCTCTCGGC-3'
KDSR G271E-R	5'-GCCGAGAGCATGTACTCATCTGAGCCAAGGG-3'
KDSR-F	5'-GGATCCATGCTGCTGCTGGCTGCCGCCTTCC-3'
KDSR Δ10+VSSA-R	5'-CTAGGCAGAGCTTACTTGCTGGAGCCCCTCAGTAATAGAAG-3'
KDSR E75Nfs*2-R	5'-TCAATTTTTCTTTGCCTGCAGCAGC-3'
KDSR G182S-F	5'-CAGTTGGGATTATTCAGTTTCACAGCCTAC-3'
KDSR G182S-R	5'-GTAGGCTGTGAAACTGAATAATCCCAACTG-3'

Table S5. Primer sequences used to generate *KDSR* mutant plasmids for *in vitro* experiments.

For Review Only